Designing with composite materials

Designing with Composite Materials

Projet avec des matériaux composites à base de fibres

Bemessungsgrundlagen für Faserverbund-Werkstoffe

Stephen W. TSAI
USAF Mat. Lab.
Wright-Patterson AFB
Dayton, USA

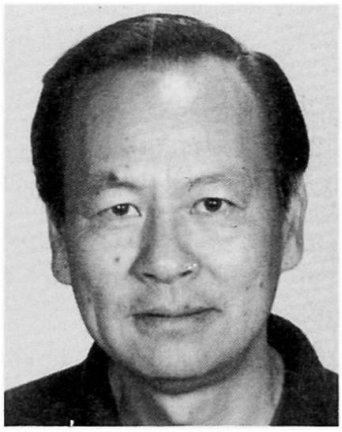

Stephen W. Tsai, born 1929, received his BE and D.Eng. degrees at Yale University, New Haven, Connecticut. He began his work in composite materials in 1961. His effort in simplifying the design process through spreadsheets, graphics, and macros is well accepted by thousands of engineers around the world.

Ajit K. ROY
Researcher
University of Dayton
Dayton, OH, USA

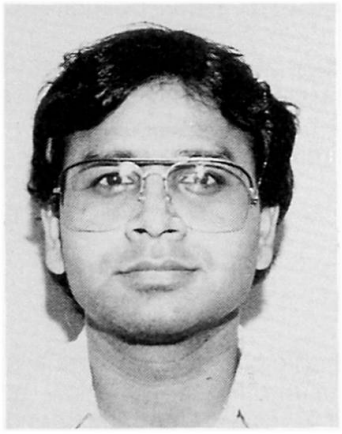

Ajit K. Roy, born 1957, received his B.Tech. degree at Indian Institute of Technology, Kharagpur, India, and MS and PhD degrees at University of Minnesota, Minneapolis, Minnesota. He is a recipient of National Research Council's Research Associate fellowship. His research interest is in analysis and design of composite structures.

SUMMARY
Ultra-high stiffness and strength fibers can be made into useful structures through laminates from unidirectional plies oriented at selected angles. Other outstanding properties of composite materials include forty percent lighter than aluminum, high endurance limit, high corrosion resistance, and novel fabrication and assembly techniques. Cost, joining, and inspection are some of the negative factors. Design process has been arbitrary and inconsistent. It is the intent here to outline our approach to design which should make composite structures, large or small, reliable and cost effective.

RÉSUMÉ
Des fibres de rigidité et de résistance extrêmement élevées peuvent être transformées en des structures utiles par l'intermédiaire de couches laminées unidirectionelles orientées selon certains angles. D'autres propriétés extraordinaires de ces matériaux composites comprennent un poids de quarante pourcent inférieur à celui de l'aluminium, une limite d'endurance élevée, une résistance à la corrosion élevée, ainsi que des techniques nouvelles de fabrication et de montage. Les coûts, l'assemblage et l'inspection sont quelques-uns des facteurs négatifs. L'étude du projet a été jusqu'ici arbitraire et irrationelle. L'intention de cet article est de montrer une approche du projet qui devrait rendre les structures composites – grandes ou petites – fiables et économiques.

ZUSAMMENFASSUNG
Fasern hoher Festigkeit und sehr hoher Steifigkeit können in Laminaten mit geeignet ausgerichteten Fasern nutzbringend Verwendung finden. Andere hervorragende Eigenschaften dieser Verbundmaterialien sind die Gewichtseinsparung von 40 % gegenüber Aluminium, die hohe Dauerhaftigkeit, die Korrosionsbeständigkeit und neuartige Herstellungs- und Montagetechniken. Hohe Kosten, die Notwendigkeit des Zusammenfügens und die Ueberwachung sind einige der negativen Faktoren. Die Bemessung geschah bisher mit fallweisen, nicht widerspruchsfreien Annahmen. Es wird hier der Versuch unternommen, ein Bemessungsvorgehen aufzuzeigen, welches Verbund-Bauelemente, seien sie gross oder klein, zuverlässig und kostengünstig werden lässt.

1. INTRODUCTION

Composite materials have been recognized as viable engineering materials for numerous applications in the aerospace industry. The stiffness of unidirectional and laminated composites is predictable and can be applied to structures with confidence. The strength, on the other hand, is empirical and continues to improve as basic data, particularly those under combined stresses, become available. It is the purpose of this presentation to cover some of the recent developments in the prediction of the strength of the laminated composite. With more reliable strength prediction the design process can be simplified considerably, and the degree of empiricism and subjective judgement can be reduced proportionally.

Glass fibers were found to possess unusually high strength many years ago. Many structures have been made from fiberglass, the first modern composite material, since the 1940's. Greater applications of fiberglass continue to emerge, including those for large buildings and nearly every sporting good from canoes to tennis rackets. Glass fibers have one glaring deficiency: low Young's modulus. Until boron fibers were discovered in the late 1950's, the stiffness required for aircraft structures limited materials to various aluminum alloys. Boron fibers made from a vapor deposition process became the first "advanced composite" which could produce structures with stiffness comparable to that of aluminum. Later graphite fibers, made from polyacrylic nitrile fibers through heating and stretching, made composite materials more competitive than aluminum. Later Du Pont's aramid fibers, with a trade name of Kevlar, emerged with the lowest density of all fibers fit for structural applications. More recently new organic fibers continue to emerge. One example is the polyethylene fiber, which is lighter that water.

Unidirectional fibers are combined into unidirectional plies or woven into fabric forms for further processing. The plies and fabric may be preimpregnated with matrix materials. The plies and fabric can be placed over one another to form multidirectional laminates. This process is often done by hand, but some automated layup machines are available. Other popular processing methods include:

Filament-winding of pressure vessels and pipes where either "prepreg" or wet winding can be used. The latter process puts resin on the fiber bundle before it is placed on a mandrel.

Pultrusion of simple and complicated cross-sections where fibers are pulled through dies.

Numerous compression, injection and transfer molding processes developed for reinforced and unreinforced plastics.

2. BASIC STIFFNESS AND STRENGTH DATA

Elastic constants and strengths of orthotropic plies in x-y plane are usually based on four constants (longitudinal, transverse and shear moduli and Piosson's ratio), and five strength data (longitudinal tensile and compressive strengths X and X', transverse tensile and compressive strengths Y and Y', and longitudinal shear strength S).

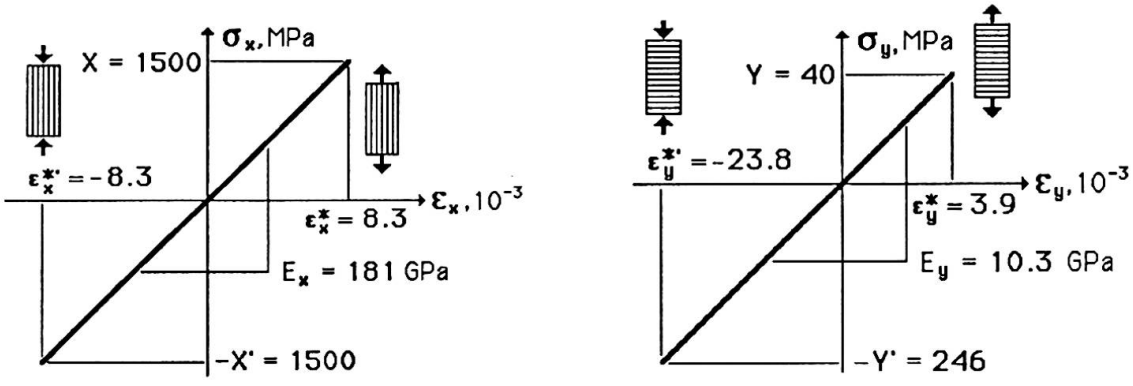

Figure 1 Uniaxial tensile and compressive stiffnesses and strengths of [0] and [90] T300/5208 graphite/epoxy composite material.

In the following table, such data for typical composites are listed. All of the orthotropic stiffnesses and strengths of each composite are also listed. Of the composite materials listed, the first eight are unidirectional plies; the last two are woven fabric.

Table 1 Stiffnesses, fiber volume, specific gravity, unit ply thickness, and strengths of various composite materials

Type	CFRP	BFRP	CFRP	GFRP	KFRP	CFRTP	CFRP	CFRP	CCRP	CCRP
Fiber/cloth	T300	B(4)	AS	E-glass	Kev 49	AS 4	IM6	T300	T300	T300
Matrix	N5208	N5505	H3501	epoxy	epoxy	PEEK	epoxy	Fbrt 934	Fbrt 934	Fbrt 934
Ply eng'g constants and data						APC2		4-mil tp	13-mil c	7-mil c
Ex,GPa	181.0	204.0	138.0	38.6	76.0	134.0	203.0	148.0	74.0	66.0
Ey,GPa	10.30	18.50	8.96	8.27	5.50	8.90	11.20	9.65	74.00	66.00
nu/x	0.28	0.23	0.30	0.26	0.34	0.28	0.32	0.30	0.05	0.04
Es,GPa	7.17	5.59	7.10	4.14	2.30	5.10	8.40	4.55	4.55	4.10
v/f	0.70	0.50	0.66	0.45	0.60	0.66	0.66	0.60	0.60	0.60
rho	1.60	2.00	1.60	1.80	1.46	1.60	1.60	1.50	1.50	1.50
ho,mm	0.125	0.125	0.125	0.125	0.125	0.125	0.125	0.100	0.325	0.175
Quasi-isotropic constants										
E,GPa	69.68	78.53	54.84	18.96	29.02	51.81	78.35	56.24	52.67	47.07
nu	0.30	0.32	0.28	0.27	0.32	0.30	0.30	0.32	0.32	0.32
G,GPa	26.88	29.67	21.35	7.47	10.95	19.88	30.23	21.37	19.89	17.8
Max stress, MPa										
X	1500	1260	1447	1062	1400	2130	3500	1314	499	375
X'	1500	2500	1447	610	235	1100	1540	1220	352	279
Y	40	61	51.7	31	12	80	56	43	458	368
Y'	246	202	206	118	53	200	150	168	352	278
S	68	67	93	72	34	160	98	48	46	46
Max strain, eps E-03										
x	8.29	6.18	10.49	27.51	18.42	15.90	17.24	8.88	6.74	5.68
x'	8.29	12.25	10.49	15.80	3.09	8.21	7.59	8.24	4.76	4.23
y	3.88	3.30	5.77	3.75	2.18	8.99	5.00	4.46	6.19	5.58
y'	23.88	10.92	22.99	14.27	9.64	22.47	13.39	17.41	4.76	4.21
s	9.48	11.99	13.10	17.39	14.78	31.37	11.67	10.55	10.11	11.22

Comparing directionally dependent properties, it is difficult to judge the relative merits of composite materials. It is a common practice to compare the longitudinal properties of composite materials against one another, as well as against isotropic materials like aluminum and steel. Such comparisons are not useful because composite materials are not usually used in unidirectional forms subjected to uniaxial tensile loads. In most cases, bidirecional loads are encountered. Laminated composites having several ply orientations are required. Fortunately for each stiffness component that varies drastically with ply orientation there is an invariant, a constant that is associated with the area under the curve, shown in

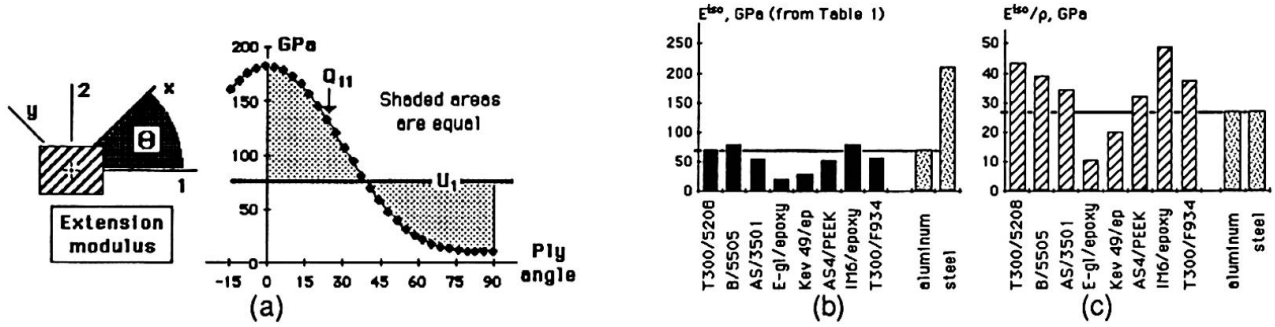

Figure 2 (a) The angular dependency of a typical stiffness component, and its associated invariant U_1.
(b) Effective quasi-isotropic constants of various composite materials, and aluminum and steel.
(c) The same quasi-isotropic stiffness normalized with respect to specific gravity.

Figure 2(a). For each orthotropic material listed in Table 1 we list the equivalent quasi-isotropic constants. It is more meaningful to compare these isotropic constants, on an absolute basis in Figure 2(b); and on a relative basis in Figure 2(c). These comparisons are conservative because we have not claimed the advantage of directional properties which depend on the applied load, and the specific laminate stacking sequence. Suffice to say, the comparisons here make composite materials look less attractive than when the longitudinal properties are used, but they represent the minimum advantages of composite materials.

3. EXAMPLES OF APPLICATIONS

After the discovery of boron filaments in the 1960's, US Air Force began many programs to promote aircraft structures made of composites. The F-111 horizontal stabilizer was the first flight-worthy composite component.

Production of composite stabilizer for the F-14 in the early 1970's was another major milestone. That was followed by the composite stabilator for the F-15, and composite rudder and stabilizer for the F-16. In the early 1980's, Boeing 767 used nearly two tons of composite materials in its floor beams and all of its control surfaces. The USSR giant transport, Antonov 124, have a total of 5500 kg of composite materials, of which 2500 kg are graphite composites. The all-composite fin box of the Airbus Industrie A310-300 is an impressive structure in its simplicity. Nearly all emerging aircraft have extensive use of composites; examples include the Dassault-Breguet's Rafale, Saab-Scania JAS-39 Gripen, and the European Fighter Aircraft (EFA) of Britain, West Germany, Italy, and Spain.

An all-composite toe plane was built here in Helsinki about ten years ago. The Beech Aircraft's Starship 1 is another all-composite airplane, and is currently undergoing flight test. In 1986, another all-composite airplane that set a world record in nonstop flight around the world is the Voyager designed and built by Burt Rutan and his coworkers. The plane was ultra light as expected. But it also showed amazing toughness and resilience against many stormy encounters. High strength graphite composites are used in the dual rudders of the revolutionary 12-meter yacht, the USA, of the St. Francis Yacht Club's entry to the America's Cup challenge. Both the Voyager and the USA have converted composite materials from a high technology domain into household words. High visibility is an important ingredient for the growth and acceptance of composite materials as viable engineering materials.

There are other unique features offered by composite materials which have no counterpart in metals. Shear coupling, for example, is a built-in characteristic of an off-axis or unbalanced laminate. Aeroelastic tailoring is an application of the shear coupling characteristic such that an airfoil can be tuned to control the bending /twisting ratio. Composites can also possess zero or negative expansion coefficients. The characteristic is utilized to build dimensional stable structures such as microwave antennas.

Materials and processing advances have been instrumental to the growth of our technology. Graphite and aramid fibers became commercially available in the early 1970's. Epoxies are available for various use conditions. More recently, higher temperature matrix materials and thermoplastics have emerged for more demanding applications of the future.

In the mean time, the high technology of composites has spurred applications outside the aerospace industry. The sporting goods is a major outlet of our material. Hundreds of tons of graphite composites were used for tennis and squash rackets, and golf shafts each year since 1983. These rackets and composites are synonymous. Applications in other than boats and rackets include bicycles, oars for rowing, and just about any equipment where weight, stiffness, and strength are important.

Examples of large structures using composite materials are limited at this time. Space structures can be large. So can off-shore drilling platforms where a number of applications are being investigated. The tethers for tension leg platform (TLP), the risers, and the legs of fixed platforms are possible future applications. US Army has built mobile bridges using composite materials.

At a conference held by the Engineering Society of Detroit's conference in December 1985, an automotive industry executive saw the impact of composite materials on the automobile industry to be as great as if not greater than that of electronics. Such high expectation of composites is good for our

technology. The acceptance of composites can be greatly enhanced if the cost is lowered; the design, simplified. We would like to address primarily the design issue which is intimately related to the cost.

4. INTEGRATED MICRO-MACROMECHANICS ANALYSIS

Micromechanics is used to relate the properties of fiber and matrix to those of a unidirectional ply. There are many analytic models for this purpose, but we recommend a modified rule-of-mixtures relation shown in the following figures:

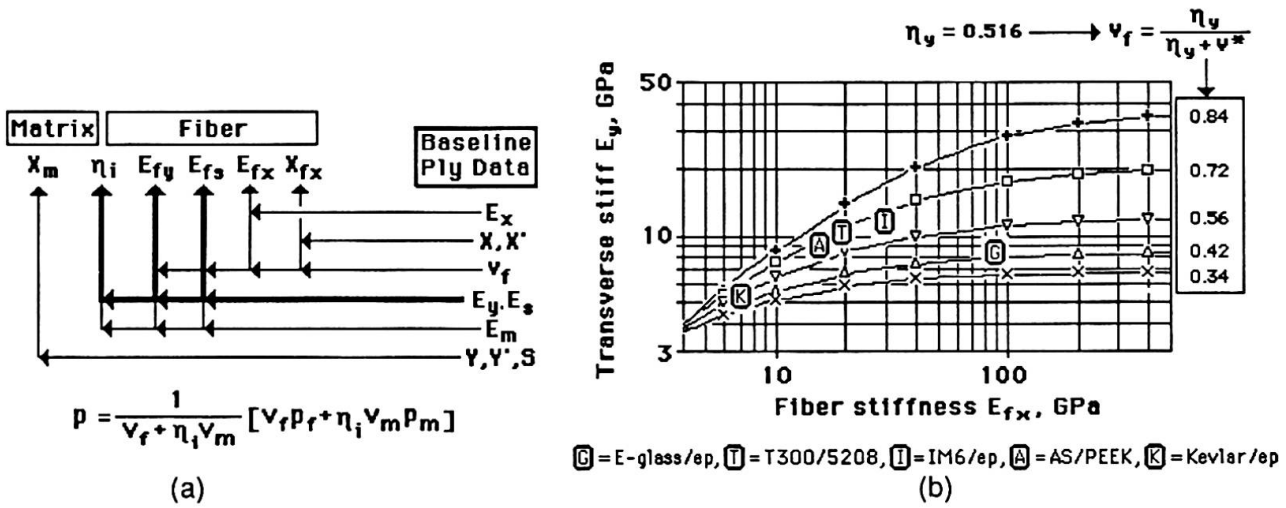

Figure 3 (a) The back-calculated fiber and matrix stiffnesses from the baseline ply data, and the modified rule-of-mixtures formula.
(b) The result of this micromechanics model showing the transverse stiffness as a function of fiber transverse stiffness, volume fraction and the stress-partitioning parameter etc. The position occupied by typical composite materials having epoxy matrices are also shown.

The powerful integrated micro- and macromechanics analysis is achieved by combining the micromechanics, such as the one recommended above, with the classical laminate plate theory, examples for the latter with be shown in the next section. With an integrated micro-macromechanics model, we can show the contribution of the constituent properties to those of the resulting composite material. Thus composite laminates can be optimized from selecting the best combination of the constituents and ply orientations. The additional dimension in materials design is unique with composite materials. The integrated micro-macromechanics model simplifies the design process.

5. STIFFNESS OF SYMMETRIC LAMINATES

The simplest form of multidirectional composites is a symmetric laminates subjected to in-plane and flexural loads. For the in-plane loads case, we usually assume that the strain across the laminate thickness is constant. This is shown in Figure 4(a). The resulting stress in each ply will be piece-wise constant, as shown in Figure 4(b). We then only need to calculate the effective laminate stiffness which is simply the rule-of-mixtures relation or the average stiffness across the laminate thickness. This is shown in Figure 4(c). These effective constants can be used directly in the stress analysis of symmetric laminates subjected to any boundary conditions, just like the case for isotropic plates.

The effective Young's modulus along any axis of a laminate must be systematically calculated using laminate plate theory. As indicated in Figure 4(c) we must take the average of the plane stress modulli [Q] to find the in-plane stiffness [A]*. By matrix inversion we find the compliance [a]*. Then engineering constant such as the Young's modulus along the 1-axis is obtained from the reciprocal of the appropriate compliance component. It is therefore impossible to guess the value of the resulting engineering constant. The parallel spring model does not work.

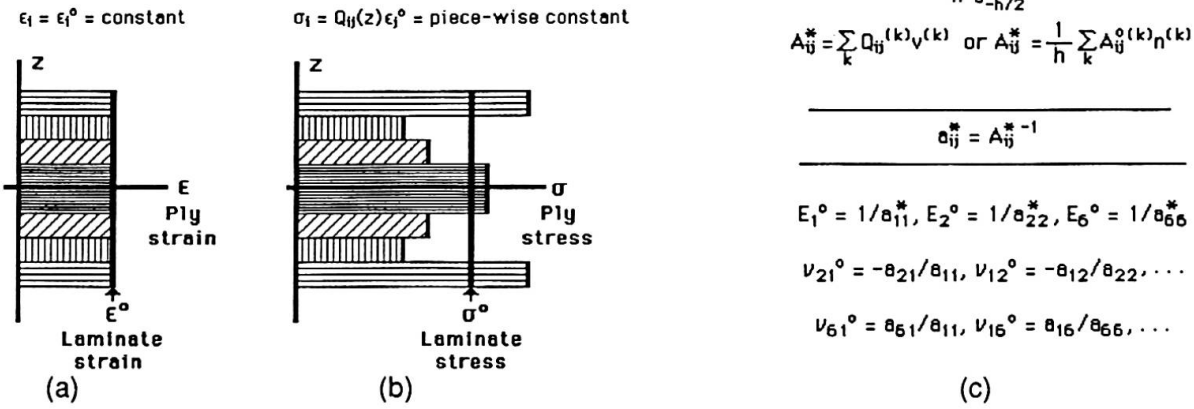

Figure 4 (a) The assumed constant laminate strain across the laminate thickness.
(b) The variation of ply stresses resulting from different ply orientations.
(c) The effective in-plane laminate constants for symmetric laminates.

In Figure 5(a), it is shown that the difference between an off-axis Young's modulus of a unidirectional composite is significantly different from that of an angle ply. Had the parallel spring model worked, the two moduli would have been the same. In Figure 5(b) we compare the effect of angle plies on the effective Young's modulus of various common laminates. In Figure 5(c) we show the effective shear moduli as functions of various laminates.

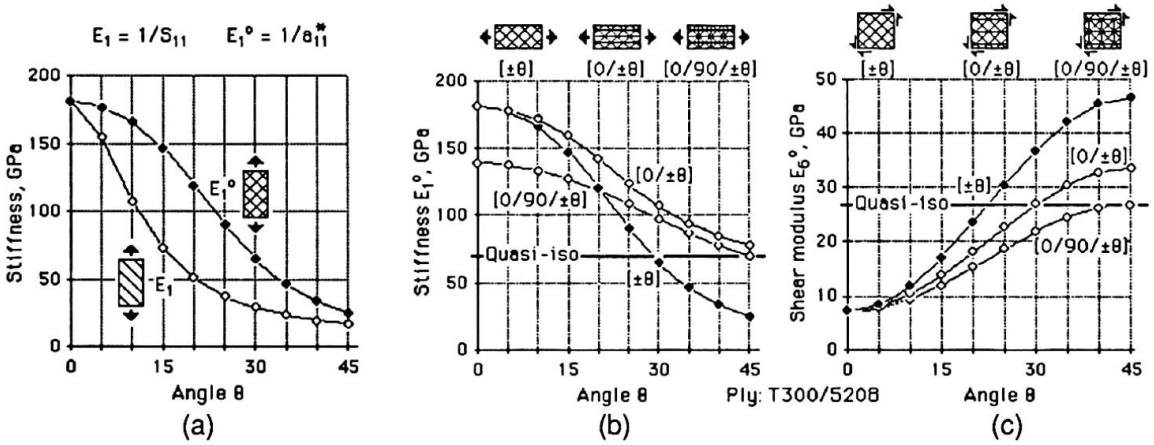

Figure 5 (a) Comparison between the Young's modulus of an off-axis unidirectional and angle-ply laminate.
(b) Young's moduli of various laminates as functions of angle-plies with different angles.
(c) Shear modulli of various laminates as functions of angle-plies with different angles.

In the case of flexural loading of a symmetric laminate, we need to assume that the strain across the thickness is a linear function of the thickness. The flexural stiffness is now a weighted average of the plies. The positions of the plies are now important. Once the flexural stiffness is known, the compliance and associated engineering constants can be derived from the same relations; i.e., the flexural compliance is obtained from the matrix inversion of the stiffness matrix, and engineering constants and coupling ratios are obtained from reciprocals and ratios of the compliance components. These relations are shown in Figure 6(a).

In Figures 6(b) and 6(c), we show the convergence of the flexural stiffness to that of the in-plane when the laminate approaches a homogenized plate with increasing repeating sublaminates. For a

T300/5208 [0/90] cross-ply laminate in Figure 6(b) the two orthogonal stiffnesses are equal. The two corresponding flexural stiffnesses converge toward that value. For laminates where the ratio of the thickness of the two angles are different from unity, say, 2 to 1 as in Figure 6(c), The flexural stiffness converges toward different values as the laminate approaches a fully homogenized state.

$$D_{ij}^{*} = \frac{12}{h^3}\int_{-h/2}^{h/2} Q_{ij} z^2 dz$$

$$D_{ij}^{*} = \frac{12}{h^3}\frac{1}{3}\sum_k Q_{ij}^{(k)}\left[(z^{(k)})^3 - (z^{(k+1)})^3\right]$$

$$d_{ij}^{*} = D_{ij}^{*-1}$$

$$E_1^f = 1/d_{11}^{*},\ E_2^f = 1/d_{22}^{*},\ E_6^f = 1/d_{66}^{*}$$

$$\nu_{21}^f = -d_{21}/d_{11},\ \nu_{12}^f = -d_{12}/d_{22},\ \cdots$$

$$\nu_{61}^f = d_{61}/d_{11},\ \nu_{16}^f = d_{16}/d_{66},\ \cdots$$

(a)

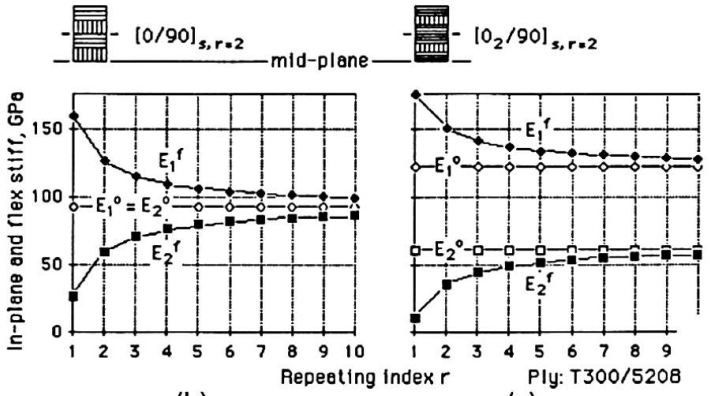

(b) (c)

Figure 6 (a) Flexural stiffness, compliance and engineering constants of a symmetric laminate.
(b) Convergence of the Young's modulus in flexure toward that in in-plane of a [0/90] laminate.
(c) Same as (b) for a different cross-ply laminate.

6. FAILURE ENVELOPES

From Table 1 we showed that the strengths of composite materials, like the stiffnesses, are highly directionally dependent. It would be optimistic to compare the longitudinal strength of unidirectional composite with that of an isotropic material unless the composite materials is used to carry uniaxial tensile load. Since composite materials are weak in carrying biaxial loads, laminates of multidirectional plies are made to achieve biaxial strength. Of all possible multidirectional laminates, the quasi-isotropic laminate represents the minimum performance of the composite material. It is therefore a conservative basis for comparing various composite materials as well as with isotropic materials.

In Figure 7(a) we show the relative longitudinal strength of various composite materials with aluminum. This comparison is optimistic. A better comparison is shown in Figure 7(b) where the quasi-isotropic strength is compared with that of aluminum. This comparison is further normalized with respect to the relative specific gravities of aluminum over that of the composite material. Note that many CFRP's have strength advantages over aluminum between 10 to 50 percent.

The ply strengths in the principal stress plane, and the corresponding ultimate strains in the principal strain space can be mapped. All failure criteria envelopes must pass through these four strength points. These points are shown in Figure 7(c), for T300/5208, whose ply properties are listed in the first column of Table 1.

Having those four points, various failure criteria can be drawn through these points to represent the strength of a composite material under the influence of combined stresses.

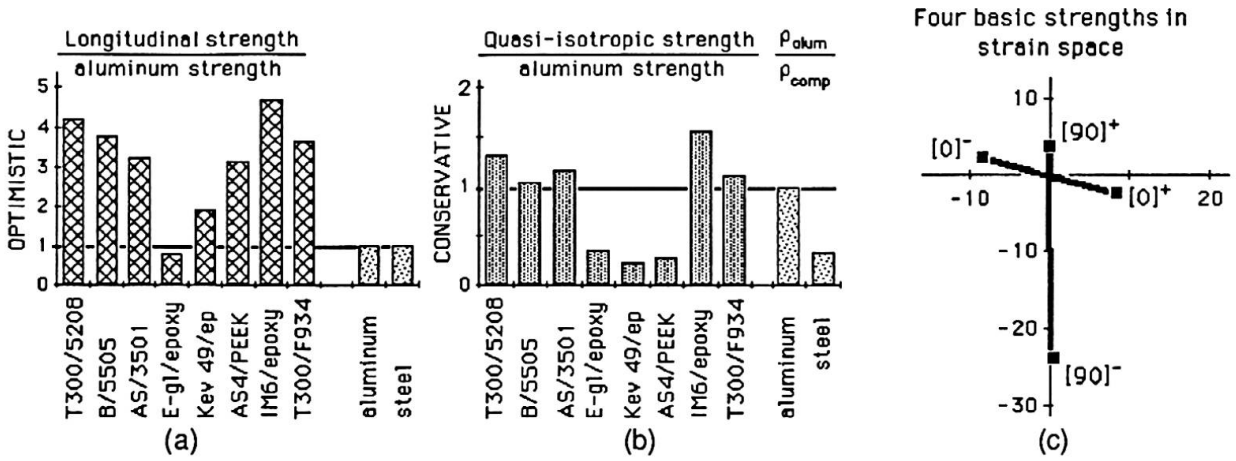

Figure 7 Basic strength comparisons, in (a) and (b), and (c) four basic strengths plotted in strain space.

The failure criterion of isotropic material is most frequently described by the von Mises criterion which is based on a scalar product (a quadratic invariant), and is fully interactive. The same criterion can be shown in strain space. The scalar product or quadratic criteria can be applied to orthotropic material in two as well as three dimensional stresses or strains. For a transversely isotropic material, which is an accurate representation of a unidirectional composite, the resulting criterion is straight forward:

Quadratic criterion in stress space:

$$F_{ij}\sigma_i\sigma_j + F_i\sigma_i = 1 \qquad F_{xx}\sigma_x^2 + 2F_{xy}\sigma_x\sigma_y + F_{yy}\sigma_y^2 + F_{ss}\sigma_s^2 + F_x\sigma_x + F_y\sigma_y = 1$$

$$F_{xx} = \frac{1}{XX'},\ F_{yy} = \frac{1}{YY'},\ F_{ss} = \frac{1}{S^2},\ F_x = \frac{1}{X} - \frac{1}{X'},\ F_y = \frac{1}{Y} - \frac{1}{Y'}$$

$$F_{xy} = \text{interaction term} = F_{xy}^{*}\sqrt{F_{xx}F_{yy}}$$

For closed conic surfaces: $-1 \le F_{xy}^{*} \le 1$

Quadratic criterion in strain space:

$$G_{ij}\epsilon_i\epsilon_j + G_i\epsilon_i = 1 \qquad G_{xx} = F_{xx}Q_{xx}^2 + 2F_{xy}Q_{xx}Q_{xy} + F_{yy}Q_{xy}^2$$

$$\vdots$$

$$G_y = F_xQ_{xy} + F_yQ_{yy}$$

Figure 8 Formulation of quadratic failure criteria in stress and strain spaces.

In Figure 9 we show quadratic failure envelopes as functions of the normalized interaction term. All envelopes must pass through the four basic uniaxial strengths shown in Figure 7(c). The degree of interaction will determine the best fit envelope among the possible shapes shown in Figure 9. Biaxial test data are required for the determination of this interaction term. A number of experimental methods are available for this purpose.

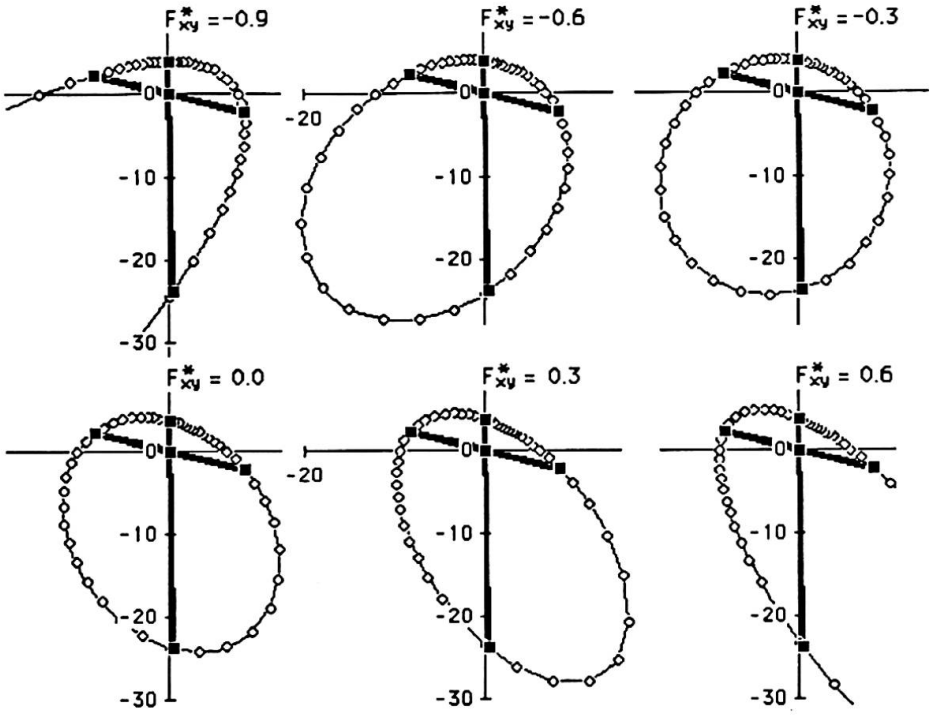

Figure 9 Various possible failure envelopes for T300/5208 as functions of the interaction term.

7. FIRST-PLY FAILURE ENVELOPES

When multidirectional plies are bonded together to form a laminate the effective stiffness of the laminate and the stresses and strains in each ply can be calculated using classical laminated plate theory. From the resulting ply stress or ply strain the failure criterion can be used to determine the strength of the

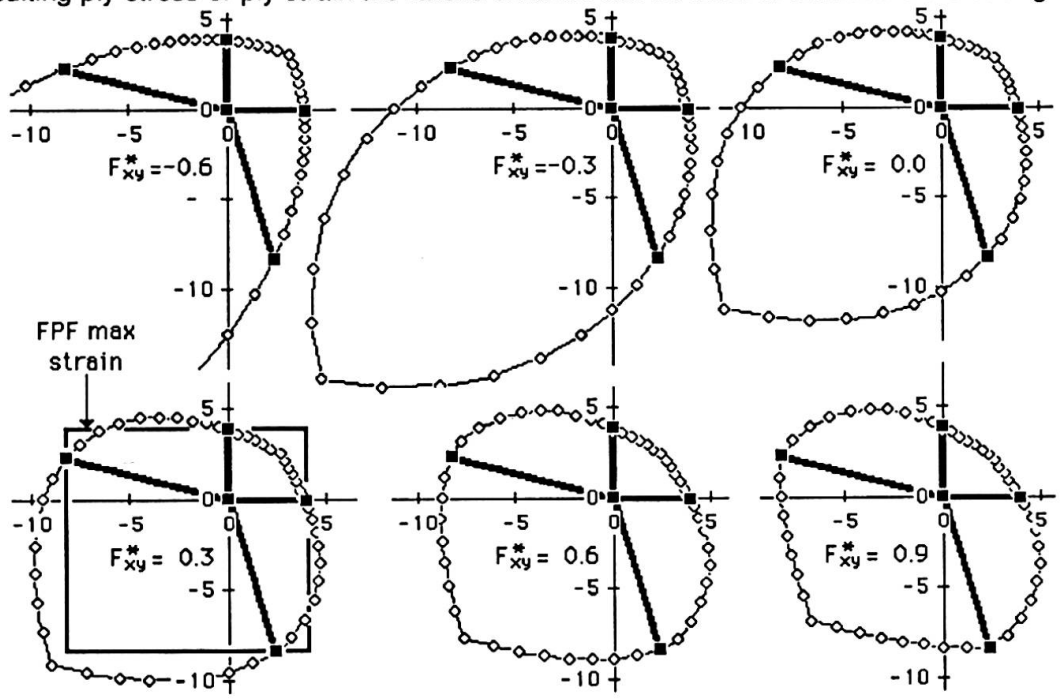

Figure 10 Various first-ply-failure envelopes for T300/5208 as functions of the interaction term.

laminate. Following the pattern of Figure 9 where failure envelopes of a unidirectional composite as functions of the interaction term are plotted, we show in Figure 10 the inner envelopes of a [π/4] laminate:

8. SENSITIVITY OF THE INTERACTION TERM

The effect of the interaction term of the quadratic failure criterion on the failure envelopes of [π/4] laminate is shown in Figure 10 for T300/5308. The range of variation goes from -0.6 to 0.9, at intervals of 0.3.

The four anchor points in the FPF envelopes above are the transverse tensile failure and longitudinal compressive failure for [0] and [90]. The [45] and [-45] do not control in the principal strain plane for this composite material. As a comparison, the FPF based on the maximum strain criterion is simply a box drawn through those four anchor points. A value of 0.3 for the interaction term in the figure above will approximately match the quadratic and maximum strain failure envelopes.

9. LAST-PLY-FAILURE

The use of laminated plate theory beyond the first-ply-failure is not strictly valid because matrix/interface failures in the form of periodically dispersed cracks begin to reach a saturation level. Laminated plate theory is valid for continuous media; i.e., where cracks do not exist. However, the laminated plate theory can be used for predicting the Last-Ply-Failure(LPF) by a simple empirical method as illustrated in the following stress-strain diagram:

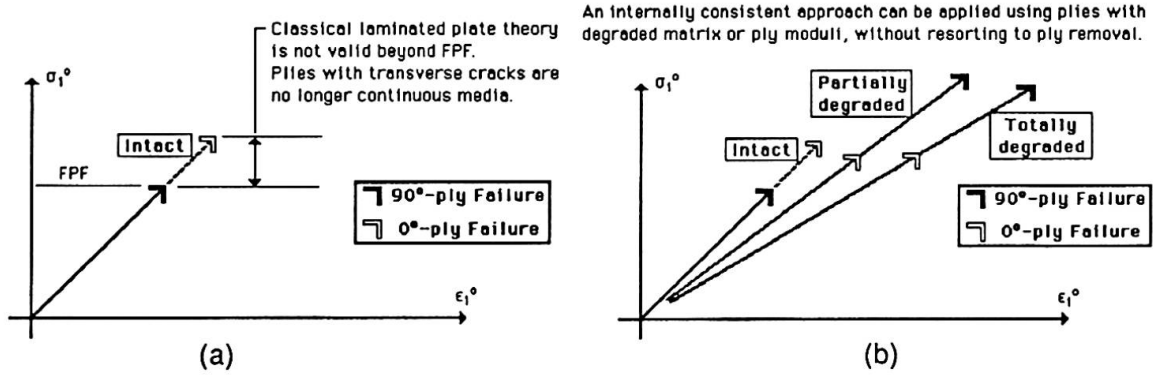

Figure 11 Schematic stress-strain curves of [0/90]s laminate for various degrees of damage. The ply failures for each degree of damage are also indicated.

If an applied uniaxial load is first applied to the [0/90]s laminate beyond the FPF and then is decreased to zero and reloaded, we would expect the stress-strain curve to follow the partially degraded curve with a reduced laminate stiffness because of the cracking of the 90 degree ply as shown in Figure 11(b). The laminated plate theory can be used to predict the macroscopic failure with an degradation of the matrix stiffness for the 90 degree ply. We assume that the ultimate strength or Last-Ply-Failure(LPF) of a laminate is reached when all plies are saturated with transverse cracks, and the prediction of the LPF is

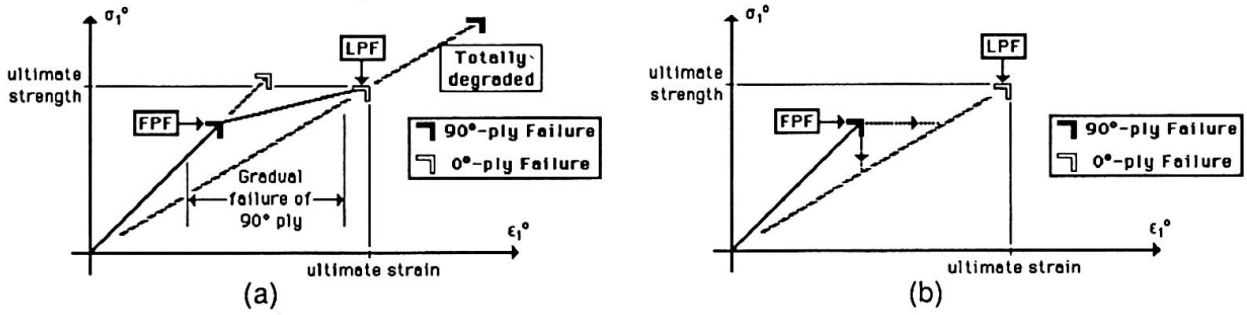

Figure 12 (a) Simplified prediction of the LPF based on the laminate with totally degraded plies.
(b) Loading path beyond the FPF for load and displacement controlled tests.

corresponding to the total degradation of all plies and the ply with the lowest failure load corresponds to the ultimate strength of the laminate. For design purposes, the FPF and LPF are important. Thus, and for convenience of computation, the partially degraded model is ignored. This simplified approach is shown in Figure 12.

The transition between the FPF for the intact plies to the eventual LPF along the degraded plies depends on many factors. The path can be idealized as a horizontal line if the loading machine is load controlled. If the machine is displacement controlled, the path can be idealized as a sudden drop in the load, followed by increase along the stiffness of degraded plies, as shown in Figure 12(b). In actual testing, the transition is smooth because the stiffness between the intact and degraded plies is small. For example, for practical laminates, the loss of laminate stiffness due to total matrix degradation is less than 10 percent. We therefore recommend a smooth transition shown in Figure 12(a). If the applied load increases monotonically, the stress-strain curve is expected to follow the intact line, then deviate from the FPF point to the LPF point on the totally degraded line. Thus, the key for the determination of the last-ply-failure is the degradation factor.

10. DEGRADATION FACTOR

It is simple to introduce a method of describing plies with cracks by using continuous plies with lower matrix stiffness. This is shown in the following:

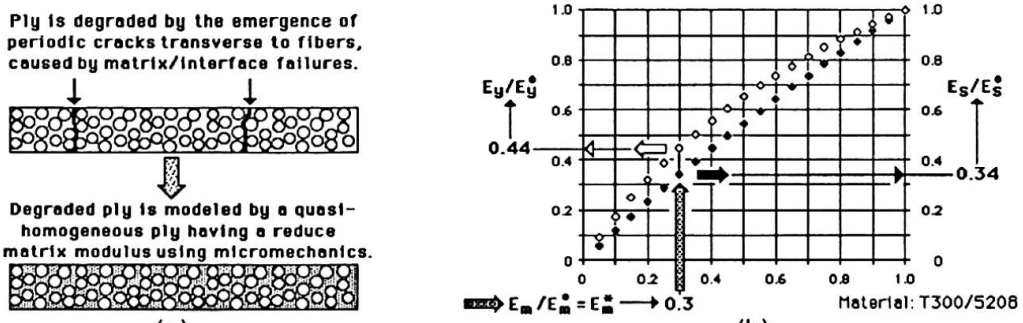

Figure 13 (a) Replacement of degraded plies by quasi-homogeneous plies.
(b) Relative reduction in transverse and shear moduli due to reduction in matrix stiffness.

The cracked plies are replaced with a continuum of quasi-homogeneous plies of lower stiffness so that the conventional stress analysis can be applied. Using a simplified micromechanics formula, based on the stress partitioning parameters, we can show the reduced transverse and shear stiffnesses resulting from a reduced matrix modulus. In the above Figure 13(b), as an example for T300/5208, for a fractional degradation of matrix stiffness to 0.3 the corresponding reduction in transverse stiffness and shear stiffness are to 44 and 34 percent respectively.

In summary, the FPF and LPF are related by the matrix degradation factor; the FPF is for the intact ply or when the degradation factor is unity. When the degradation factor decreases the shape of the failure envelope changes. Failure envelopes and failure strengths of [π/4] laminates with various degree of degradation are shown in Figure 14(a):

In Figure 14(a) the failure envelopes are obtained using the quadratic failure criterion as discussed in section 6. It is shown in this figure that when the value of the matrix degradation factor approaches to zero, the failure envelope converges to that of the maximum strain or netting analysis. Thus in the limiting case the results of maximum strain or netting analysis can be recovered from the quadratic criterion.

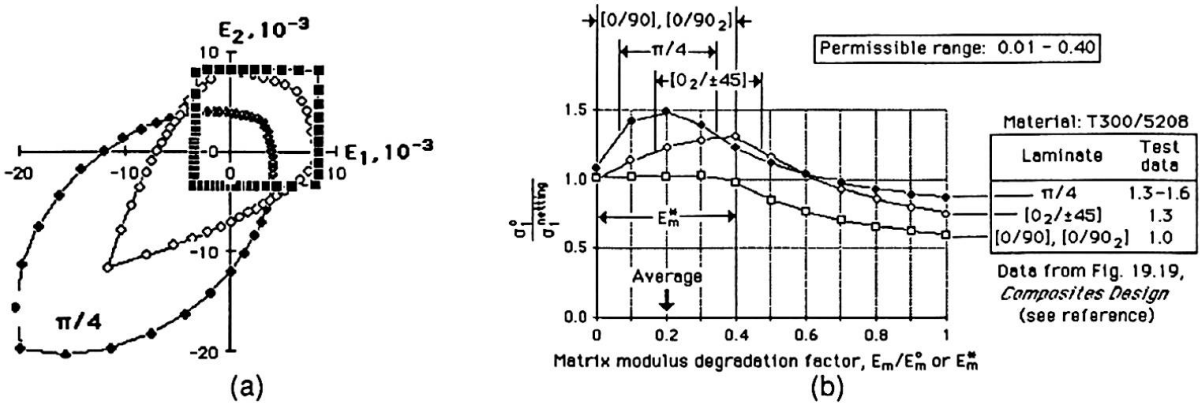

Figure 14 (a) Failure envelopes of [π/4] laminate for several degradation factor, solid diamond for E_m^*=1.0, intermediate for E_m^*=0.3, and rectangle is the netting analysis with E_m^*=0.001.
(b) Normalized tensile failure strength of several laminates versus matrix degradation factor. Comparison with test data are also shown.

11. DETERMINATION OF DEGRADATION FACTOR

The degradation factor can be determined from test data obtained from laminates. In Figure 14(b) the tensile strength calculated based on quadratic criterion for various values of the degradation factor is normalized by that of netting analysis. The tensile strength prediction by netting analysis is the product of ply tensile longitudinal strength and the fraction of [0] plies in the laminate. In the limit when the degradation factor approaches zero, the netting analysis prediction, as shown above, should prevail. For most composite materials, such extent of degradation is not likely to occur. In this figure, test data from various laminates are used to select the most probable value for the degradation factor. Assuming that the ultimate tensile strength of a laminate is equal or higher than than that of the netting analysis and comparing the test data, Figure 14(b) suggests that, for T300/5208, a value between 0.01 and 0.40 for the matrix degradation factor is permissible. An exact value is not critical for the prediction of the LPF envelope. A summary of the values of the degradation factors for typical composite materials that can be used in predicting the LPF is shown as follows:

Table 2 Degradation of stiffness and strength based on matrix degradation.

Degrade	T300/52	IM6/epoxy	AS4/PEEK	E-gl/epoxy	Kev/epoxy
E_m	3.40	3.40	3.40	3.40	3.40
E_m^*	0.20	0.10	0.10	0.07	0.02
E_y	10.30	11.20	8.90	8.27	5.50
E_y^*	0.31	0.14	0.17	0.07	0.05
E_s	7.17	8.40	5.10	4.14	2.30
E_s^*	0.27	0.11	0.16	0.08	0.06
X'	1500	1540	1100	610	235
X'*	0.77	0.64	0.70	0.60	0.57
ν_{xy}^*	0.20	0.10	0.10	0.07	0.02
$(F_{xy}^*)^*$	0.20	0.10	0.10	0.07	0.02

* means fractional degradation from intact to degraded matrix.
Longitudinal compressive strength are degraded, not linearly, but to the 0.2th power; i.e., $X'^* = [E_s^*]^{0.2}$.
Poisson's ratio and interaction term in the quadratic failure criterion are linearly degraged with the matrix stiffness.

12. RULE-BASED LIMIT AND ULTIMATE STRENGTHS

Using the degradation factor, the FPF and LPF envelopes can be obtained in a consistent manner. For T300/5208, with a factor of 0.3 for the LPF, we can show these two envelopes:

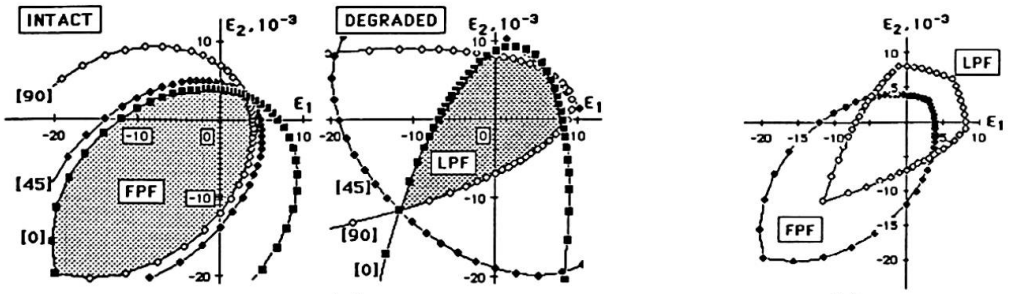

Figure 15 (a) Failure envelopes of a [π/4] laminate before and after degradation.
(b) FPF and LPF envelopes together after superposition.

Now we can establish a rule-based design criterion. These rules depend on the relative values of FPF, LPF, and the desired factor of safety. We would like to recommend the following rules:

Rule 1: ultimate strength = MAX(FPF, LPF)

Rule 2: limit* strength = ultimate/safety factor

Rule 3: limit strength = MIN(FPF, limit*)

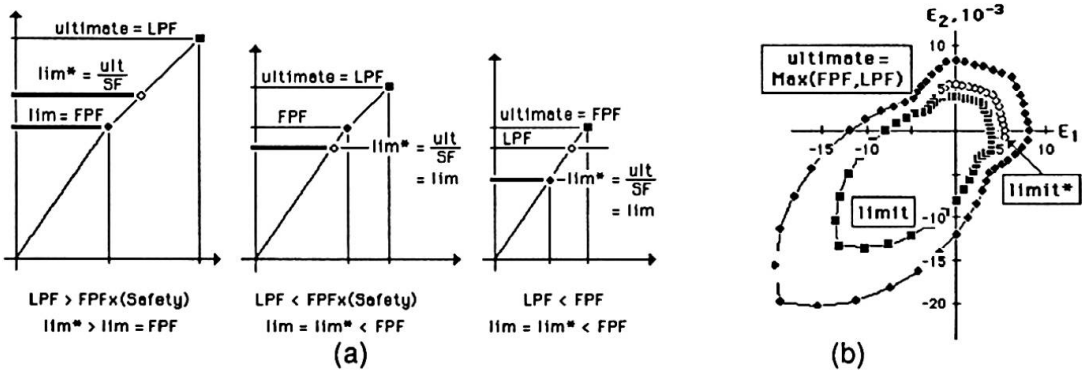

Figure 16 (a) Illustration of ultimate, limit*, and limit strengths.
(b) Ultimate, limit*, and limit failure envelopes for T300/5208 with a safety factor of 1.5.

Limit* is an ultimate based strength where matrix/interfacial cracks are tolerated; e.g., in filament-wound pressure vessels. Limit strength is more conservative where stresses beyond FPF are not permitted. However, at the same time, the limit strength takes full account of post-FPF capability to provide the maximum desired safety. These rules are shown in the Figure 16(a) above. With these rules, the ultimate, limit* and limit envelopes, with a safety factor of 1.5, are shown for T300/5208 in Figure 16(b).

13. SIMPLE DESIGN METHODS

The above mentioned design rules can easily be implemented in any design method. We would like to discuss, for example, two such simple design methods that are being used by engineers in sizing composite structural components.

13.1 Mic-Mac Spreadsheet

This is an integrated micro-macromechanics analysis, or Mic-Mac for short, which can be best performed using one of several spreadsheets now available in all personal computers. The example presented

below is based on Microsoft Excel for the Apple Macintosh computer, which can be transferred to Lotus 123 for the IBM PC computer.

	READ ME	Theta 1	Theta 2	Theta 3	Theta 4		Ply mat	T3/N52[SI]	
stacking	[ply angle]	**0.0**	**90.0**	**45.0**	**-45.0**	[repeat]	h, *	h, E-3	[Rotate]
	[ply*]	**1.0**	**1.0**	**1.0**	**1.0**	**1.0**	8.0	1.0	**0.00**
strength ratios	R/intact	0.598	0.325	0.383	0.383	R/FPF	0.325	safety	**1.50**
	R/degrade	0.559	0.618	0.974	0.974	R/LPF	0.559	R/lim*	0.373
						R/ult	0.559	R/lim	0.325
loads & laminate moduli	{N}, MN/m or k/in	{N}lim	{N}lim*	{N}ult	{E°}lim	E^ul/E^lr	<alph>E-6	<beta>	
	compon't1	**1.00**	0.325	0.373	0.559	69.68	0.91	1.52	0.0401
	compon't2	**0.00**	0.000	0.000	0.000	69.68	0.91	1.52	0.0401
	compon't6	**0.00**	0.000	0.000	0.000	26.88	0.89	0.00	0.0000
stresses & strains at limit,et al.		<sg°>	<sg°>lim	<sg°>lim	<sg°>ult	<ep°>E-3	<ep°>lim	<ep°>lim*	<ep°>ult
	compon't1	1000	325	373	559	14.35	4.67	5.91	8.87
	compon't2	0	0	0	0	-4.25	-1.38	-1.87	-2.81
	compon't6	0	0	0	0	0.00	0.00	0.00	0.00
micromech variables		T opr	c,moist	vol/f	Em	Efx	Xm	Xfx	Em/Em°
	Baseline	22.0	0.005	0.70	3.40	259	40.0	2143	0.20
	[Modified]	**22.0**	**0.005**	**0.70**	**3.40**	**259**	**40.0**	**2143**	**0.20**
	Mod/Base	1.000	1.000	1.000	1.000	1.000	1.000	1.000	1.000

Figure 17 Example of Mic-Mac spreadsheet for designing composite structural components.

The eminent feature of the Mic-Mac spreadsheets is that all the micromechanics and macromechanics variables are integrated together by the interlinked cells of the spreadsheets. Thus designers can immediately see the effect of any micromechanics variable on the final design and this tool is extremely useful for the sensitivity study of any design variable.

13.2 Design by Ranking

Another method of design can be based on ranking of a family or families of sublaminates. The use of sublaminates in design has two major advantages. One, splicing of the total laminate with a number of sublaminates reduces manufacturing cost and is less prone to make mistake in lamination. Two, instead of having all the plies of same angles stacked up together, if the laminate is made up with sublaminates, the interlaminar stresses can be reduced and consequently the laminate will be stronger against delamination.

Number of plies	2 orientations	3 orientations	4 orientations
2	3	6	10
3	4	10	20
4	5	15	35
5	6	21	56
6	7	28	84
7	8	36	120
8	9	45	165
9	10	55	220
10	11	66	286
Total	65	285	1000

(a)

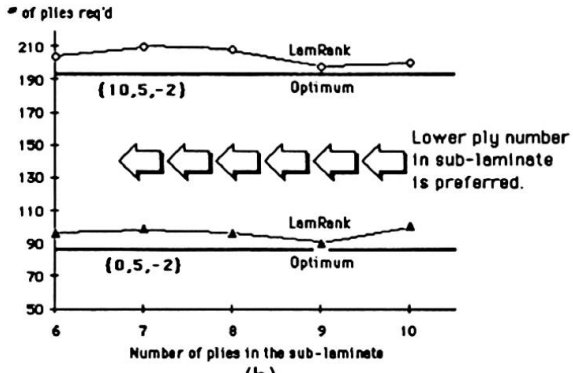

(b)

Figure 18 (a) Number of sublaminates in a family for given number of ply orientation and plies.
(b) Influence of number of plies in a sublaminate on the design thickness of the laminate for two load cases.

A large number of sublaminates can be ranked in optimizing a laminate. The number of sublaminates in a laminate family is a function of the number of plies and number of orientations in a sublaminate. Figure 18(a) shows the number of possible sublaminates in a family of given number of orientations

(between 2 and 4) and total number of plies (between 2 and 10). It is shown in Figure 18(b) that, for six or more number of plies in a sublaminate, the laminate ranking method can yield virtually an optimum laminate.

14. CONCLUSIONS

We have shown an approach to extend the common failure criteria from the FPF to LPF using a matrix degradation factor. Then rules for design can be based on limit* or limit, using any value of safety factor. This approach can be illustrated in the following flow diagram:

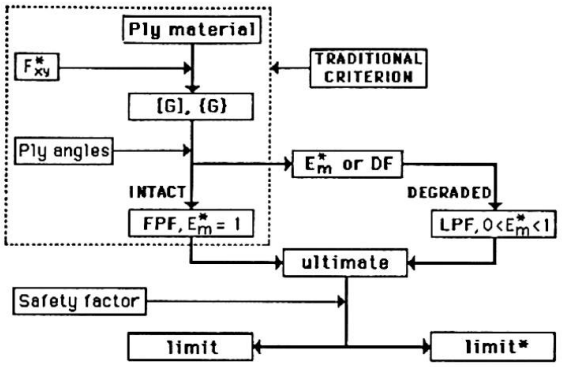

Figure 19 Flow chart of a laminate design.

While we recommend the quadratic criterion, but the approach outlined here can be applied to any other failure criteria. The only change necessary will be replacing the [G] and {G}, the strength parameters in strain space by whatever appropriate parameters corresponding to the chosen failure criterion.

The degradation factor proposed here is preferred over the ply removal method. It is also preferred over complete degradation; i.e., assigning a value approaching zero. The stiffness of a degraded structure can also be used to estimate the degree of degradation.

We believe the approach that we propose is simple, easy to understand, and easy to compute. It is internally consistent, and extend the utility of laminated plate theory for the prediction of the LPF of a laminate. This approach is better than using two unrelated models; e.g., laminated plate theory for FPF, and netting analysis for the burst pressure. Much work remains to be done for the proposed approach.

The experimental data are always difficult to assemble. But with a framework such as ours, we believe that the critical data can be obtained systematically.

REFERENCE

Stephen W. Tsai, *Composites Design*, 3rd ed, Think Composites, Dayton (1987).

Leere Seite
Blank page
Page vide